Time Delay of the Resistive-State Formation in Superconducting Stripes Excited by Single Optical Photons

Recently proposed superconducting single-photon detectors (SSPD's), based on ultrathin, submicrometer-width NbN superconducting stripes, are characterized by picosecond response times, high quantum efficiency, broadband single-photon sensitivity, and extremely low dark counts.[1,2] The devices have immediately found a variety of applications ranging from noninvasive testing of very-large-scale integrated (VLSI) circuits[3] to quantum cryptography.[4,5] Their single-photon-counting ability has been interpreted within a phenomenological hot-electron photoresponse model proposed in Ref. 1 and elaborated in Ref. 6. The model describes the formation of a hotspot,[7] right after the single-photon absorption event, followed by in-plane growth of a resistive hotspot area due to the high efficiency of the excited quasiparticle multiplication process in NbN films.[8] During this stage, however, the resistive state does not appear across the superconducting stripe because the size of a single normal hotspot, created by an optical photon, is significantly smaller than our stripe width.[2] The resistive state appears due to a supplementary action of the device's bias current density j, which should be close to the stripe's critical current density j_c. After the supercurrent is expelled from the normal hotspot region, the bias current density in the stripe's "sidewalks" j_{sw} exceeds j_c [see Fig. 92.32(c)], resulting in the penetration of the electric field in the sidewalk areas of the stripe.[6] As a result, we observe a voltage pulse that reflects the initial act of photon capture.

The resistive-state development process presented above should lead to an experimentally observable time delay in the superconducting stripe's resistive photoresponse.[9] This delay, in turn, if measured, would give direct confirmation of a supercurrent-enhanced, hotspot-induced photoresponse mechanism of our SSPD.[1]

The dynamics of the resistive-state formation in a photon-illuminated, two-dimensional (2-D) superconducting stripe depends on the radiation flux density incident on the device and the bias current density, as is schematically illustrated in Fig. 92.32. At relatively high (macroscopic) incident photon fluxes, a large number of hotspots are simultaneously formed in our superconducting stripe [Fig. 92.32(a)]. In this case, the hotspots overlap with each other across a cross section of the stripe. Since the stripe thickness d is comparable with coherence length ξ, we can assume that for overlapping hotspots, a resistive barrier is instantaneously formed across the NbN stripe and, as a result, a voltage signal is generated within an electron thermalization time of 6.5 ps.[10] When the photon flux is decreased, the hotspots become isolated [Fig. 92.32(b)]. Finally, for the flux containing one or less than one absorbed photon per pulse, we can expect that, at best, only one resistive

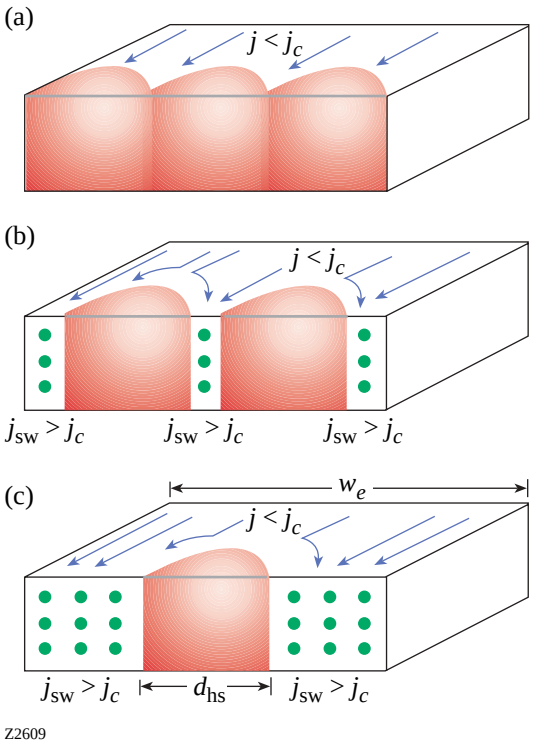

Figure 92.32
Schematic presentation of the dynamics of resistive-barrier formation across a superconducting stripe: (a) high (macroscopic) incident photon flux, (b) the two-photon regime, leading to the generation of two hotspots in the cross section of the superconducting stripe, and (c) the single-photon regime.

hotspot will be formed in our stripe [Fig. 92.32(c)]. As we mentioned above, in the single-photon regime, we postulate that the formation of a macroscopic resistive barrier can be realized only when j_{sw} surpasses j_c, which is associated with macroscopic current redistribution and should lead to a certain time delay in the resistive-state formation.

Even if the two-photon detection mechanism[1,2] does not correspond exactly to the situation presented in Fig. 92.32(b) since the hotspots can either partially overlap or coincide, the scenario illustrated in Fig. 92.32(b) should result in a measurable time delay t_d for the voltage pulse generation, corresponding to the time period between the initial hotspot appearance and the eventual development of a resistive barrier across the entire cross section of the superconducting stripe. In terms of the superconductor dynamics, t_d is the time required for a superconductor energy gap Δ to be reduced to zero by the current in the sidewalks and, for $j_{sw} > j_c$, can be calculated using the Tinkham model[11] as

$$t_d = 2\tau_\Delta \int_0^1 \frac{f^4}{\left[2j_{sw}/\left(3\sqrt{3}j_c\right)\right]^2 + f^6 - f^4}\, df, \qquad (1)$$

where $\tau_\Delta \cong 2.41\tau_E/\sqrt{1-T/T_c}$ is the gap relaxation time[9] (τ_E is the inelastic electron–phonon collision time at the Fermi level at T_c) and $f = \Delta/\Delta_0$ ($\Delta_0 = \Delta$ at 0 K).[11]

The devices used in our experiments were 4×4-μm^2-area, meander-type, NbN stripes with d = 10 nm, a nominal width w = 130 nm, and the total length of about 30 μm. The structures were superconducting at T_c = 10.5 K and exhibited $j_c = 6 \times 10^6$ A/cm^2 at 4.2 K. Details of their fabrication and implementation as SSPD's are described in Refs. 2 and 4; here we only wanted to stress that with the constant j_c, I_c of the meander is determined by its narrowest segment, and, according to our supercurrent-enhanced, resistive-state formation model, the narrowest segments of the stripe contribute the most to the SSPD photoresponse.[2] The atomic force microscope images showed that irregularities in our stripes were up to 25 nm, close to the cantilever resolution limit. At the same time, the I_c of the meander structures, measured at 4.2 K, was typically 60% lower than I_c for the control (short) stripe fabricated in the same process. Thus, to account for the width variations, we introduce the effective stripe width w_e, corresponding to the detector segments most active in the resistive-state formation and photon detection, and we estimate w_e to be 80 nm.

Our devices were mounted inside a cryostat on a cold base plate maintained at 4.2 K, wire-bonded to a 50-Ω microwave stripe line, and connected to the bias and output circuitry through a cryogenic bias-tee.[4] As optical excitation, we used 100-fs-wide pulses from a Ti:Al_2O_3 laser with a wavelength of 810 nm and a repetition rate of 82 MHz. The laser radiation power was attenuated down to a picowatt range using banks of neutral-density filters. Voltage pulses generated by our SSPD's were amplified directly by a room-temperature amplifier and fed to a synchronously triggered Tektronix 7404 single-shot digital oscilloscope, or they were counted by a fast electronic counter. The photon counter was used to determine the single-photon, two-photon, or multiphoton regimes of operation of our devices, as described in detail in Refs. 1 and 2. The amplifier and the oscilloscope had bandwidths of 0.01 to 12 GHz and 0 to 4 GHz, respectively. Thus, the ~100-ps real-time resolution of our entire readout system was determined mainly by the oscilloscope performance. On the other hand, digital averaging procedures of acquired pulses allowed us to achieve the relative-time resolution (e.g., delays between the photoresponse pulses generated under different photon excitations) of ~5 ps, due to extremely low intrinsic jitter in our measurement system.

Figure 92.33 presents the measured time delays in the photoresponse signal versus the number of absorbed photons, calculated as the photon flux density incident upon the meander multiplied by the device detection efficiency (DE).[2] The data are presented for two experimental bias conditions at $j/j_c = 0.85$ (open circles) and $j/j_c = 0.6$ (closed circles) and correspond to the SSPD single-photon and two-photon regimes of operations, respectively.

We will discuss the single-photon $\left(j/j_c = 0.85\right)$ regime first, remembering that for our 4×4-μm^2 device, DE for counting single, 810-nm photons at $j/j_c = 0.85$ is ~10^{-3} (Ref. 2). We observe that for large absorbed photon fluxes (macroscopic number of photons per pulse) t_d does not depend on the radiation flux. Clearly, this situation corresponds to the multi-hotspot-generation case presented in Fig. 92.32(a). We will use this condition as a reference and refer to it as $t_d = 0$. When the incident flux is decreased to about 10 absorbed photons/pulse, the arrivals of the photoresponse signals start to be time delayed with respect to the multiphoton response and t_d increases. Subsequently, t_d saturates when the flux density is decreased down to about 10^{-1} absorbed photons/pulse. In this case, we are in the single-photon counting mode [Fig. 92.32(c)]. Thereafter, the arrival of the photoresponse pulse is not further delayed in time scale even if we attenuate

the flux down to 10^{-3} absorbed photons/pulse. We interpret the measured time interval between the multiphoton and the single-photon responses, Δt_d = 65±5 ps, as the time needed for supercurrent redistribution around a single, photon-created hotspot and subsequent formation of the resistive barrier for $j_{sw} > j_c$.

We repeated the same experiment, but with a significantly lower bias current applied to the detector (curve $j/j_c = 0.6$ in Fig. 92.33). In this case, according to Ref. 2, the probability of detecting a single, 810-nm photon by our 4×4-μm^2 device is negligibly small; thus, at least two photons are needed to generate the resistive response. As seen in Fig. 92.33, the observed behavior (closed circles) is very similar to that measured for $j/j_c = 0.85$; we can clearly identify the time-delay phenomenon and find Δt_d = 70±5 ps. The main difference is that the observed photoresponse delay is now shifted into significantly higher levels of the incident photon flux. The value of t_d starts to be nonzero for ~10^3 absorbed photons/pulse, and it flattens at ~10 absorbed photons/pulse. The latter value is very consistent with the two-photon detection mechanism.[1,2]

Finally, we can compare our experimental results with t_d calculated for our experimental conditions, using Eq. (1) and $\tau_E \approx 10$ ps.[10] The current density in the sidewalks in the narrowest (most-active) segments of the meander can be calculated as $j_{sw} = j\left[w_e/\left(w_e - d_{hs}\right)\right]$, where $d_{hs} \approx 30$ nm is the diameter of the hotspot for 810-nm photons.[2] Thus, for the experimental $j/j_c = 0.6$ condition, $j_{sw}/j_c = 0.96$ and is subcritical in a single-hotspot regime. However, doubling the hotspot size[12] gives $j_{sw}/j_c = 1.28$, which is sufficient to generate a resistive barrier across our stripe. In a similar manner, when $j/j_c = 0.85$, j_{sw}/j_c is supercritical and reaches 1.36 when the single hotspot is formed. Figure 92.34 shows the t_d dependence on j_{sw}/j_c; the solid line represents the Tinkham model,[11] while the two closed circles refer to our measured Δt_d values, corresponding to the $j_{sw}/j_c = 1.36$ and $j_{sw}/j_c = 1.28$ conditions, respectively. We note that our experimental values are reasonably close to the theoretical prediction, remembering that the Tinkham theory is applicable for clean superconductors, while our 10-nm-thick NbN films are in the dirty limit. In addition, the discrepancy can be related to the accuracy of our w_e estimation.

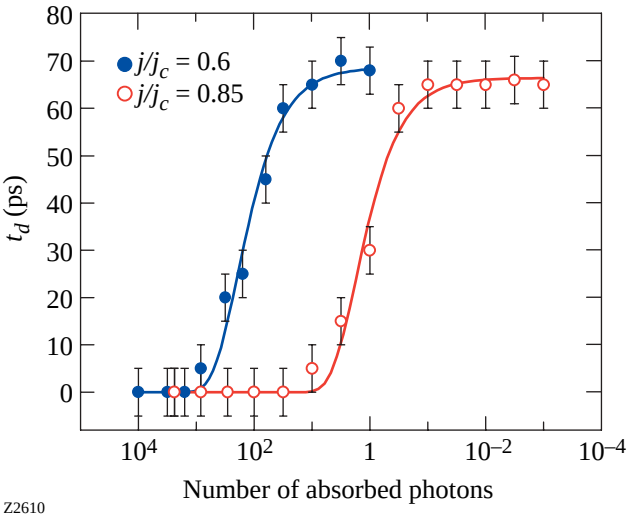

Figure 92.33
Experimental time delay t_d of the resistive-state formation in a NbN superconducting stripe as a function of the incident absorbed photon flux density. Open circles correspond to t_d measured when the stripe was biased with $j/j_c = 0.85$ (single-photon regime), and closed circles represent $j/j_c = 0.6$ and the two-photon regime. Solid lines are guides to the eye. The measurement error is ±5 ps.

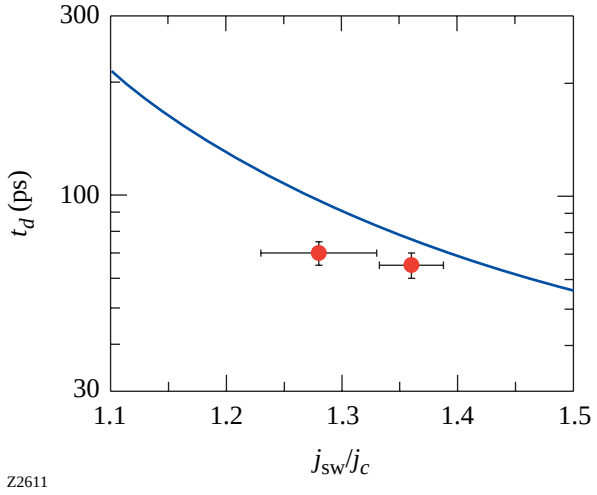

Figure 92.34
Time delay t_d as a function of the normalized current in the sidewalks of the superconducting stripe j_{sw}/j_c. The two measured values of Δt_d (solid circles) correspond to the single-hotspot and two-hotspot formation at $j_{sw}/j_c = 1.36$ and $j_{sw}/j_c = 1.28$, respectively. The solid line represents the theoretical prediction, calculated using Eq. (1), and the horizontal error bars are calculated for the hotspot-diameter variations of 30±1 nm.

In conclusion, we observed the time-delay phenomenon in the resistive-state response in ultrathin, submicrometer-width NbN superconducting stripes, excited by single optical photons. The observed phenomenon directly shows that the resistive state across an ultrathin, submicrometer-width superconducting stripe upon absorption of an optical photon is due to photon-induced hotspot formation and subsequent redistribution of the supercurrent into the sidewalks of the stripe. Our measurements agree well with a theoretical prediction based on the Tinkham model of the resistive-state formation in superconducting stripes under the supercurrent perturbation.[11]

ACKNOWLEDGMENT

The authors thank Ken Wilsher for many valuable discussions. This work was funded by the NPTest, San Jose, CA. Additional support was provided by the US Air Force Office for Scientific Research Grant F49620-01-1-0463 (Rochester) and by the RFBR grant 02-02-16774 (Moscow).

REFERENCES

1. G. N. Gol'tsman, O. Okunev, G. Chulkova, A. Lipatov, A. Semenov, K. Smirnov, B. Voronov, A. Dzardanov, C. Williams, and R. Sobolewski, Appl. Phys. Lett. **79**, 705 (2001).

2. A. Verevkin, J. Zhang, R. Sobolewski, A. Lipatov, O. Okunev, G. Chulkova, A. Korneev, K. Smirnov, G. N. Gol'tsman, and A. Semenov, Appl. Phys. Lett. **80**, 4687 (2002).

3. S. Somani, S. Kasapi, K. Wilsher, W. Lo, R. Sobolewski, and G. Gol'tsman, J. Vac. Sci. Technol. B, Microelectron. Nanometer Struct. **19**, 2766 (2001).

4. A. Verevkin, J. Zhang, W. Slysz, R. Sobolewski, A. Lipatov, O. Okunev, G. Chulkova, A. Korneev, and G. N. Gol'tsman, "Superconducting Single-Photon Detectors for GHz-Rate Free-Space Quantum Communications," to be published in SPIE's *Free-Space Laser Communication and Laser Imaging II*.

5. A. Verevkin, G. Gol'tsman, and R. Sobolewski, in *OPTO-Canada: SPIE Regional Meeting on Optoelectronic, Photonics, and Imaging* (SPIE, Bellingham, WA, 2002), Vol. TD01, pp. 39–40.

6. A. D. Semenov, G. N. Gol'tsman, and A. A. Korneev, Physica C **351**, 349 (2001).

7. A. M. Kadin and M. W. Johnson, Appl. Phys. Lett. **69**, 3938 (1996).

8. K. S. Il'in, I. I. Milostnaya, A. A. Verevkin, G. N. Gol'tsman, E. M. Gershenzon, and R. Sobolewski, Appl. Phys. Lett. **73**, 3938 (1998).

9. D. J. Frank *et al.*, Phys. Rev. Lett. **50**, 1611 (1983); D. J. Frank and M. Tinkham, Phys. Rev. B **28**, 5345 (1983).

10. K. S. Il'in, M. Lindgren, M. Currie, A. D. Semenov, G. N. Gol'tsman, R. Sobolewski, S. I. Cherednichenko, and E. M. Gershenzon, Appl. Phys. Lett. **76**, 2752 (2000).

11. M. Tinkham, *Introduction to Superconductivity*, 2nd ed., International Series in Pure and Applied Physics (McGraw-Hill, New York, 1996).

12. In a case where two hotspots are present in the film, we have taken the average effective size of the double hotspot across the cross section of the NbN stripe to be $\sqrt{2}d_{\mathrm{hs}}$ to take into account a possible overlap between the hotspots.